INTERSECTII
INTERSECTIONS
www.intersections.ro

Evaluation of the seismic safety of RC framed buildings designed according to EC-2 and EC-8

Alex H. Barbat[1], Juan C. Vielma[2] and Sergio Oller[3]

[1] *Technical University of Catalonia, Departamento de Resistencia de Materiales y Estructuras en la Ingeniería, E.T.S. de Ingenieros de Caminos Canales y Puertos, Edificio C1, Campus Norte, Jordi Girona 1-3, Barcelona, 08034, Spain e-mail: alex.barbat@upc.edu*

[2] *Lisandro Alvarado University, Av. La Salle entre Av. Las industrias y Av. Benítez, Decanato de Ingeniería Civil, Departamento de Estructuras. Barquisimeto, Venezuela e-mail: jcvielma@ucla.edu.ve*

Abstract

One of the main objectives of the design of earthquake resistant structures is to ensure that these do not collapse when subjected to the action of strong motions. Modern codes include prescriptions in order to guarantee that the behavior of the elements and the whole structure is ductile. It is especially important for the designer to know the extent of damage that the structure will suffer under a specific seismic action, described by the design spectrum. To achieve this damage there are several static and dynamic nonlinear procedures. This paper presents a procedure for nonlinear static analysis in which the maximum displacements are determined based on the condition of satisfying a minimum value of a finite element based damage index. This procedure is validated by applying incremental dynamic analysis, and is used in the assessment of the response of a set of regular reinforced concrete buildings designed according to the EC-2/EC-8 prescriptions for high seismic hazard level. The results of nonlinear analysis allows the formulation of a new seismic damage index and of damage thresholds associated with five Limit States, which are used to calculate fragility curves and damage probability matrices for the performance point of the studied buildings. The results show that the design of earthquake resistant buildings according to the prescriptions of EC-2/EC-8 not only ensures that the collapse is not reached, but also that the structural damage does not exceed the irreparable damage limit state.

KEYWORDS: ductility, over strength, behavior factor, non-linear analysis, fragility curves, objective damage index

ISSN 1582-3024

INTERSECTII
INTERSECTIONS
www.intersections.ro

1. INTRODUCTION

The main objective of the earthquake resistant design is to produce structures capable to sustain a stable response under strong ground motions. Some of the aspects of the current seismic analysis procedure allow adapting the characteristics of the non-linear structural behavior to the equivalent elastic analysis. Obviously, the formulation of these characteristics is an important task in order to obtain a satisfactory design.

Recent advances and developments in the computational tools enabled to develop and to apply more realistic analysis models to new or existent buildings and to take into account main features of the non-linear seismic behavior of structures, like constitutive laws (plasticity and damage) or large deformations. The non linear analysis has been used in the assessment of buildings designed according to specific design codes [1, 2, 3].

Among the characteristics studied in past works, some examples can be provided: displacement ductility, overstrength and behavior factor. The assessment of these characteristics is possible by applying deterministic procedures in analyzing the non-linear response of the structures subjected to static or dynamic loads. The static non-linear analysis is usually performed by using a predefined lateral load distribution which corresponds to the first mode shape. The dynamic analysis is applied using a suitable set of records obtained from the existing strong ground motion databases or from design spectrum-compatible synthetic accelerograms.

Recently, the application of the Performance-Based Design concepts required the definition of a set of Limit States, usually starting from engineering demand parameters, such as the interstory drift, the global drift or the global structural damage. These parameters allow defining damage thresholds associated with the Limit States which are applied to the calculation of the fragility curves and of the damage probability matrices used in the seismic safety assessment of the buildings.

In this paper, the seismic safety of regular framed buildings is studied using static and dynamic non-linear analysis. The static analysis is performed by means of pushover procedures while the dynamic analysis is performed using the Incremental Dynamic Analysis (IDA). For this purpose, a set of 16 reinforced concrete framed buildings was designed according to EC-2 [4] and EC-8 [5]. The buildings are regular in plan and elevation. The analysis was performed using the PLCd program [6] which allows incorporating the main characteristics of the reinforcement and of the confinement provided to the structure members. The results of the non-linear analysis allow calculating the displacement ductility, the overstrength and the behavior factors of the structures. The latter are compared with those prescribed by EC-8. The global performance of the buildings is evaluated using an objective damage index, formulated starting from the capacity

ISSN 1582-3024

curve. Finally, for the predefined damage thresholds, fragility curves and damage probability matrices are calculated.

2. DESCRIPTION AND DESIGN OF THE STUDIED BUILDINGS

A set of regular reinforced concrete moment-resisting framed buildings (MRFB), designed according to EC-2 and EC-8, characterized by the number of stories (3, 6, 9 and 12) and of spans (3, 4, 5 and 6) was used in the paper. These buildings cover a low to medium structural period range and also and relevant range of structural redundancy. The structural members of are analyzed, designed and detailed according to the EC-2 and EC-8 prescriptions for high ductility class (behavior factor equal to 5.85). The seismic demand is obtained for the B Soil type design spectrum (stiff soil) and for a peak ground acceleration of 0.3g. The geometric characteristics of the studied buildings are shown in figures 1 and 2.

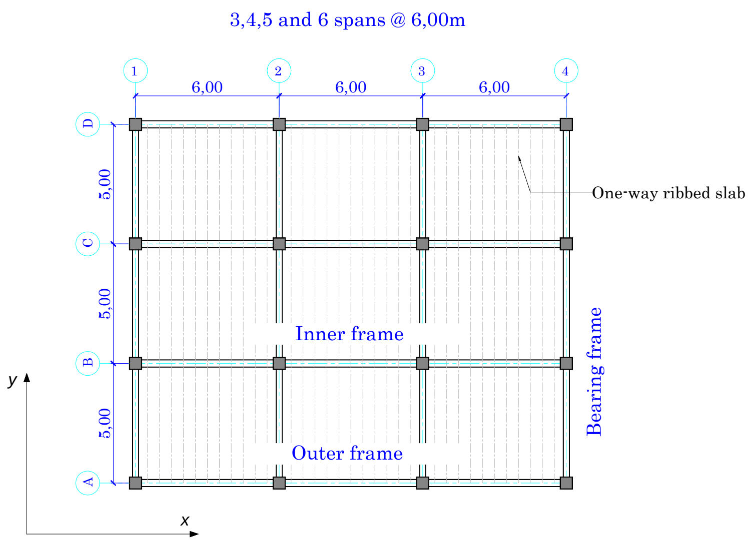

Figure 1. Plan view of the framed buildings

ISSN 1582-3024

INTERSECTII
INTERSECTIONS
www.intersections.ro

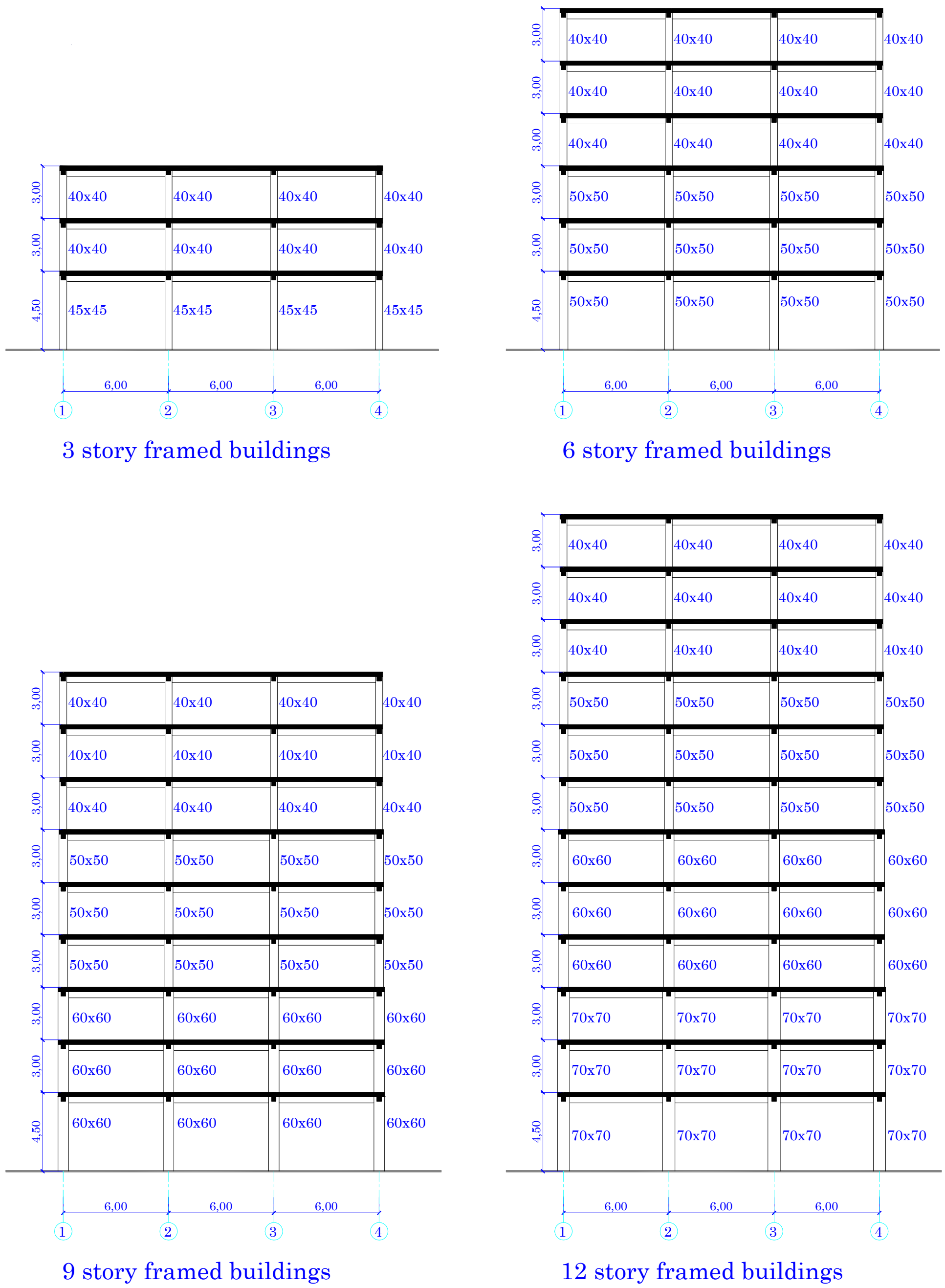

Figure 2. Elevation of the framed buildings

3. NON-LINEAR ANALYSIS OF THE BUILDINGS

3.1. Characteristics of the computational model

The non-linear static analysis with force control was performed using the PLCd finite element code [7, 8] which allows using two and three-dimensional solid elements as well as prismatic, reduced to one-dimensional, members. This code provides a solution combining both numerical precision and reasonable computational costs [9, 10]. It can deal with kinematics and material nonlinearities. It uses various 3-D constitutive laws to predict the material behavior (elastic, visco-elastic, damage, damage-plasticity, etc. [11]) with different yield surfaces to control its evolution (Von-Mises, Mohr–Coulomb, improved Mohr–Coulomb, Drucker–Prager, etc. [12]). Newmark's method [13] is used to perform the dynamic analysis. A more detailed description of the code can be found in Mata *et al.* [9,10]. The main numerical features included in the code to deal with composite materials are: 1) Classical and serial/parallel mixing theory used to describe the behavior of composite components [14]. 2) Anisotropy Mapped Space Theory enables the code to consider materials with a high level of anisotropy, without the associated numerical problems [15]. 3) Fiber–matrix debonding which reduces the composite strength due to the failure of the reinforced–matrix interface [16].

Experimental evidence shows that inelasticity in beam elements can be formulated in terms of crossectional quantities [17] and, therefore, the beam's behavior can be described by means of concentrated models, sometimes called plastic hinge models, which localize all the inelastic behaviour at the ends of the beam by means of ad-hoc force–displacement or moment–curvature relationships [18]. But, in the formulation used in this computer program, the procedure consists of obtaining the constitutive relationship at cross-sectional level by integrating on a selected number of points corresponding to fibers directed along the beam's axis [19]. Thus, the general nonlinear constitutive behavior is included in the geometrically exact nonlinear kinematics formulation for beams proposed by Simo [20], considering an intermediate curved reference configuration between the straight reference beam and the current configuration. The displacement based method is used for solving the resulting nonlinear problem. Plane cross sections remain plane after the deformation of the structure; therefore, no cross sectional warping is considered, avoiding to include additional warping variables in the formulation or iterative procedures to obtain corrected cross sectional strain fields. An appropriated cross sectional analysis is applied for obtaining the cross sectional forces and moments and the consistent tangential tensors in the linearized problem. Thermodynamically consistent constitutive laws are used in describing the material behavior for these beam elements, which allows obtaining a more rational estimation of the energy dissipated by the structures. The simple mixing rule for composition of the materials is also considered in modeling materials for these elements, which are

ISSN 1582-3024

composed by several simple components. Special attention is paid to obtain the structural damage index capable of describing the load carrying capacity of the structure.

According to the Mixing Theory, in a structural element coexist N different components, all of them subject to the same strain; therefore, strain compatibility is forced among the material components. Free energy density and dissipation of the composite are obtained as the weighted sum of the free energy densities and dissipation of the components, respectively. Weighting factors k_q are the participation volumetric fraction of each compounding substance, $k_q=V_q/V$, which are obtained as the quotient between the q-th component volume, V_q, and the total volume, V [7, 8, 9, 10].

Discretization of frames was performed with finite elements whose lengths vary depending on the column and beam zones with special confinement requirements. These confinement zones were designed according to the general dimensions of the structural elements, the diameters of the longitudinal steel, the clear of the spans and the story heights. Frame elements are discretized into equal thickness layers with different composite materials, characterized by their longitudinal and transversal reinforcement ratio (see Figure 3). Transversal reinforcement benefits are included by means of the procedure proposed by Mander *et al.* [21].

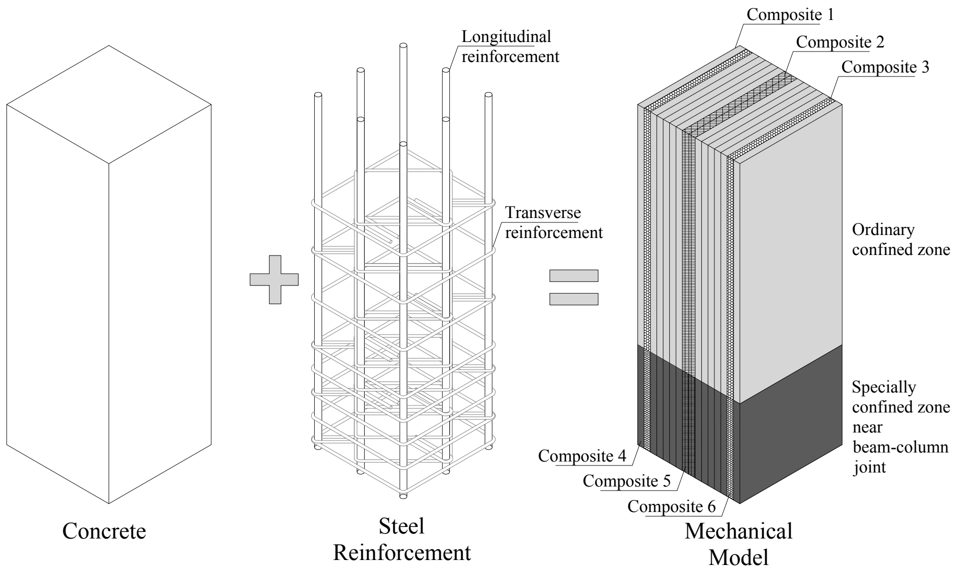

Figure 3. Discretization of the RC frame elements

INTERSECTII
INTERSECTIONS
www.intersections.ro

3.2. Non-linear static analysis

To evaluate the inelastic response of the four structures, pushover analysis was performed applying a set of lateral forces representing seismic actions corresponding to the first vibration mode. The lateral forces are gradually increased starting from a zero value, passing through the value which induces the transition from elastic to plastic behavior and, eventually, reaching the value which corresponds to the ultimate drift (*i.e.* the point at which the structure can no longer support any additional load and collapses). Before the structure is subjected to the lateral loads simulating seismic action, it is first subjected to the action of gravity loads, in agreement with the combinations applied in the elastic analysis. The method applied does not allow evaluating the effect of torsion, being the used structural model a 2D one.

Although it is difficult to find a method to obtain the global yield and ultimate displacements [22] in this work a simplified procedure is applied. The non-linear static response obtained via finite element techniques is used to generate the idealized bilinear shaped capacity curve shown in Figure 4, which has a secant segment from the origin to a point on the capacity curve that corresponds to a 75% of the maximum base shear [23]. The second segment, which represents the branch of plastic behavior, was obtained by finding the intersection of the aforementioned segment with another, horizontal segment which corresponds to the maximum base shear. The use of the compensation procedure guarantees that the energies dissipated by both nonlinear models are equal.

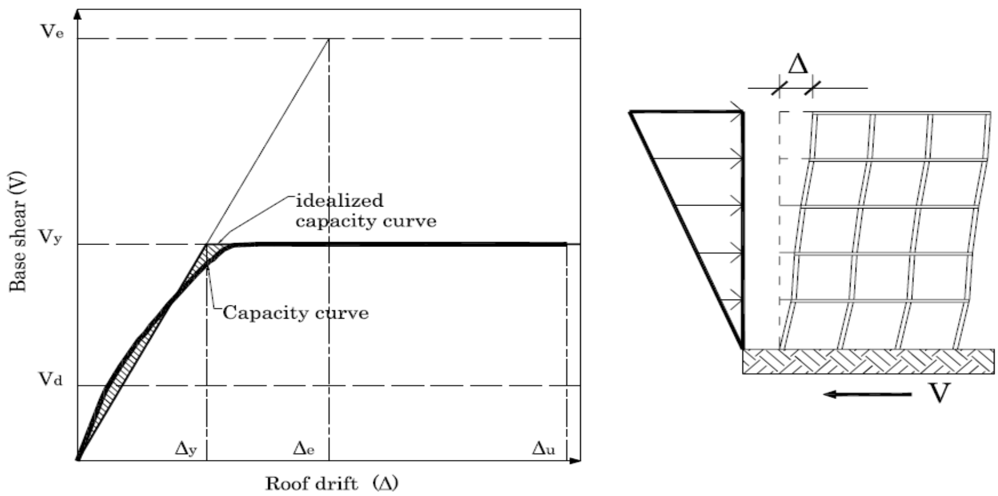

Figure 4. Scheme for determining the displacement ductility and the overstrength

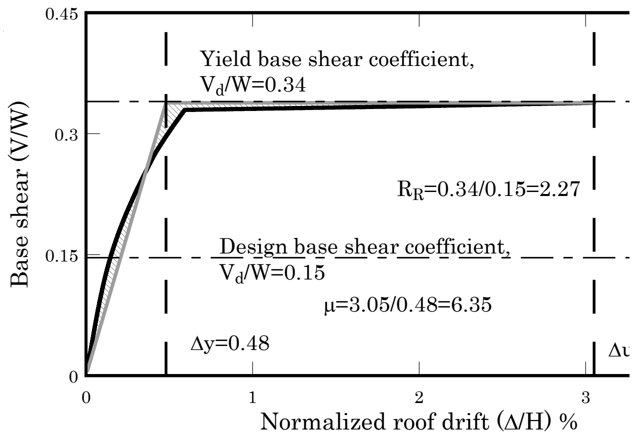

Figure 5. Idealized capacity curve of the MRFB

For simplified non-linear analysis there are two variables that characterize the quality of the seismic response of buildings. The first is the displacement ductility μ, defined as

$$\mu = \frac{\Delta_u}{\Delta_y} \tag{1}$$

and calculated based on the values of the yield drift Δy, and ultimate drift Δu, from the idealized capacity curve shown in Figure 5. The second variable is the overstrength R_R of the building, which is defined as the ration of the design base shear V_d to the yielding base shear V_y, both of which are shown in Figure 5

$$R_R = \frac{V_y}{V_d} \tag{2}$$

The overstrength R_R is like a safety factor applied in design and evaluation of the buildings.

Figure 5 shows the capacity curve of the outer frame of the 9 story building. The curve clearly illustrates how this structural type is capable to sustain stable ductile response, which is reflected in the high value for the final drift. Based on the idealized bilinear curve of this figure, a displacement ductility of 6.35 is obtained; this is a higher value than that specified in the EC-8 seismic design code, which is 5.85. In the same figure, the overstrength is also calculated, which has a value of 2.27. This means that the moment resisting buildings designed according to EC-2 and EC-8 have a ductile response to seismic forces, and also an adequate overstrength.

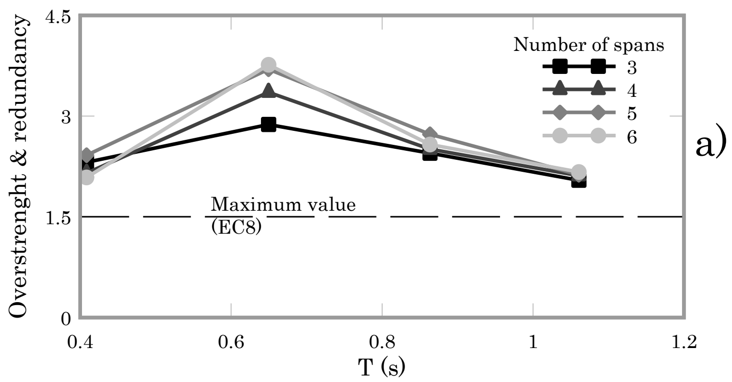

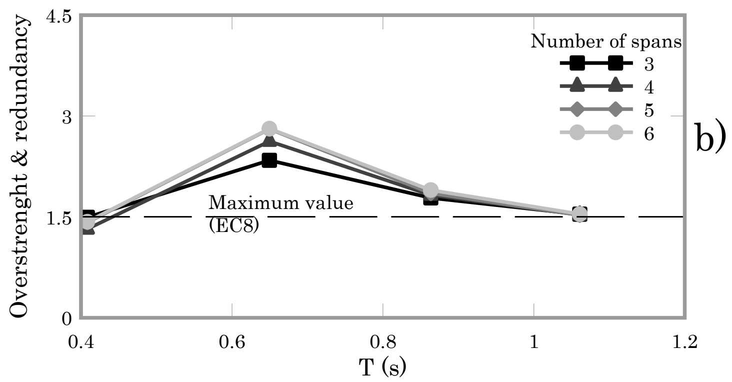

Figure 6. Overstrength and redundancy spectrum of the a) outer frames and b) inner frames

Figures 6a and 6b shows computed values of the overstrength for the outer and inner frames of the studied buildings, plotted versus the periods of the first mode, respectively. The results demonstrate clearly that influence of increasing the number of spans, which is equivalent to consider various defense lines, is very low, excepting the case of the 6 story buildings. For the other buildings, the values of the overstrength are closer. It is also seen that the computed values of the combined overstrength factors are greater than the value that EC-8 prescribes for the design of ductile framed buildings.

3.3. Damage index

A local damage index *D* is calculated using the finite element program PLCd with a damage and plasticity constitutive model that enables correlation of damage with lateral displacements [24, 25]

$$D = 1 - \frac{\left\| P^{in} \right\|}{\left\| P_0^{in} \right\|}$$

where $\left\| P^{in} \right\|$ and $\left\| P_0^{in} \right\|$ are the norm of current and elastic values of the internal forces vectors, respectively. Initially, the material remains elastic and *D=0* but, when all the energy of the material is dissipated $\left\| P^{in} \right\| \to 0$ and $D \to 1$. Figure 7 shows the distribution of the damage index to the members of the studied frames corresponding to the collapse displacement. In this figure, each rectangle represents the magnitude of the damage reached by the finite element. It is important to observe that, for low rise buildings (N=3), the maximum values of the damage occurs at the extremities of the columns of the first story; this damage concentration is characteristic for a soft-story mechanism. Instead, high rise buildings (N= 6, 9 and 12) show maximum damage values at the extremities of the beams of the stories. This is the desired objective of the conceptual design: to produce a structure with weak beams and strong columns.

It is important to know the level which the damage reaches when a structure suffers a certain demand. This is possible if the damage index is normalized respecting the maximum damage which can occur in the structure. Vielma *et al.* [26] proposed a capacity curve-based damage index D_{obj}^{P} which allows assessing the damage level for a specific roof displacement. This objective damage index $0 \le D_{obj}^{P} \le 1$ reached by a structure for a given drift corresponding to a point *P* of the capacity curve is defined as

$$D_{obj}^{P} = D_P \frac{1-\mu}{\mu} = \frac{(1 - K_P / K_0)\mu}{\mu - 1} \tag{4}$$

For example, *P* might be the performance point resulting from intersection between the inelastic demand spectrum and the capacity curve; the stiffness K_P corresponds to this point. Other parameters are the initial stiffness K_0 and the displacement ductility μ, calculated with the yield displacement Δ_y^* which

INTERSECTII
INTERSECTIONS
www.intersections.ro

corresponds to the intersection of the initial stiffness with the maximum shear value (see Figure 8).

Figure 9 shows the evolution of the objective damage index with respect to the normalized roof drift, computed for all the frames of the studied buildings.

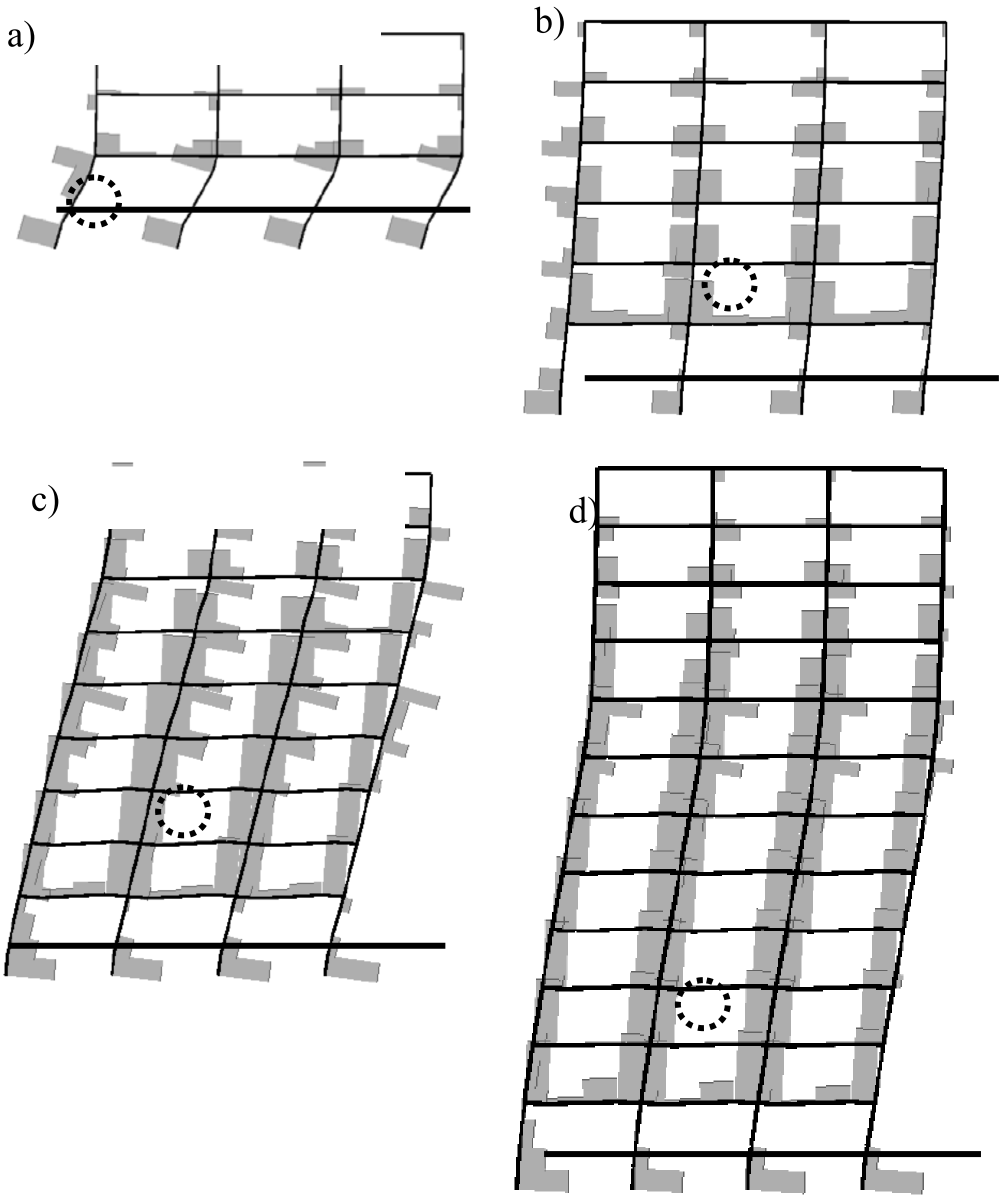

Figure 7. Distribution of the local damage index at collapse displacement

ISSN 1582-3024

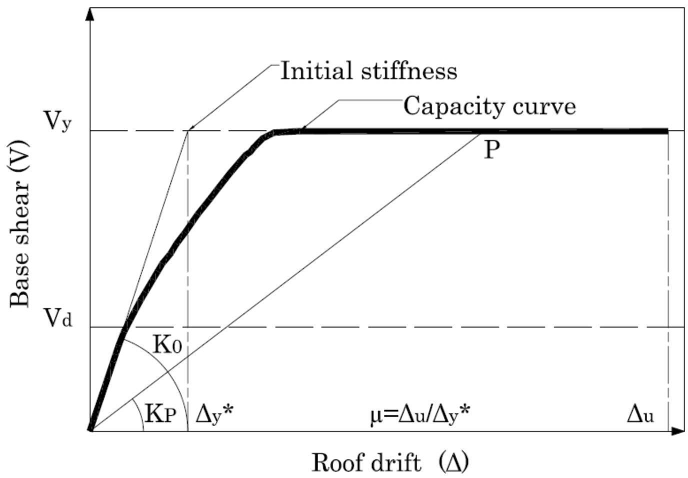

Figure 8. Parameters used in the calculation of the objective damage index

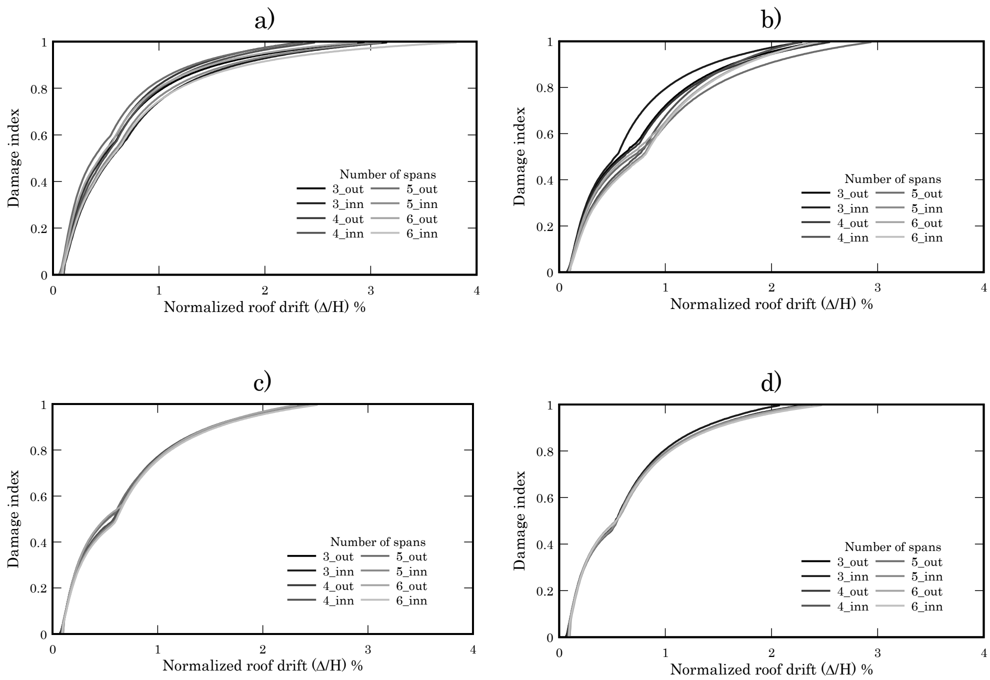

Figure 9. Evolution of the damage index of the a) 3 story, b) 6 story, c) 9 story and d) 12 story building

3.4. Incremental Dynamic Analysis

In order to evaluate the dynamic response of the buildings, the Incremental Dynamic Analysis (IDA) [27] was applied. This procedure consists in performing time-history analyses using real or artificial accelerograms, which are scaled each time in order to induce increasing levels of inelasticity in the structural model. A set of six artificial accelerograms compatible with soil type B of the EC-8 design spectrum were generated. Figure 10 shows the design spectrum and the 5% damping response spectra obtained for the set of synthetic accelerograms.

The IDA response curves are obtained plotting the ground motion intensity versus demand parameters which, in this study, are the spectral accelerations of the 5% damped spectra and the roof drifts, respectively. The collapse point is reached when the capacity of the structure drops [28]. A usual criterion is to consider the slope of the curve less than the 20% of the elastic slope [27, 29]. Figure 8 shows the IDA curves computed from the 3-spans outer frames of the 3, 6, 9 and 12 story buildings. Note that the collapse points of the frames are closer to the values of the capacity curves.

Table 2 summarizes the average values of the collapse points for all the studied cases, computed by means of the performed dynamic analysis. Dynamic analysis is useful in assessing the collapse point of the buildings and, for obtaining the values of the behavior factors q, the following equation has been proposed [2]

$$q = \frac{a_{g(collapse)}}{a_{g(design\_yield)}} \tag{5}$$

where $a_{g(collapse)}$ and $a_{g(design\_yield)}$ are the collapse and the yield design peak ground acceleration, respectively. $a_{g(collapse)}$ is obtained from the IDA curves and $a_{g(design\_yield)}$ is calculated from the elastic analysis of the building. Average values of the computed behavior factor q of the studied buildings are show in Table 2; these values correspond to the dynamic response of the buildings subjected to the set of synthetic accelerograms and are compared with the behavior factors prescribed by the design codes.

The computed behavior factors show that the applied seismic design allows designing structures with satisfactory lateral capacity when they are subjected to strong ground motions, regardless of the building height. The relationship between the calculated and the prescribed behavior factors is close to three for the case of low rise buildings.

INTERSECTII
INTERSECTIONS
www.intersections.ro

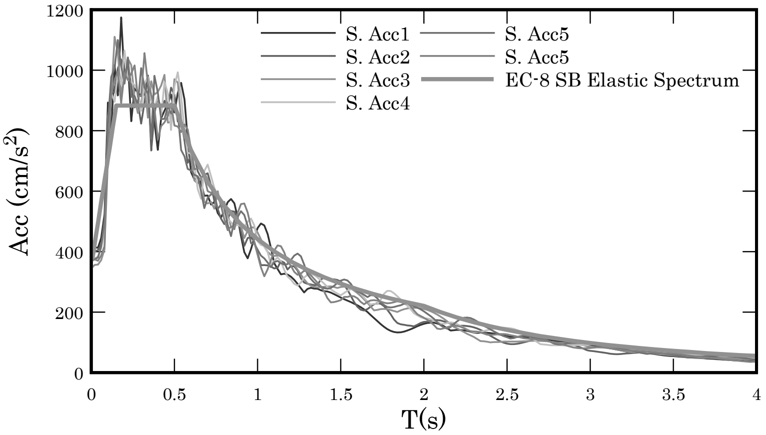

a)

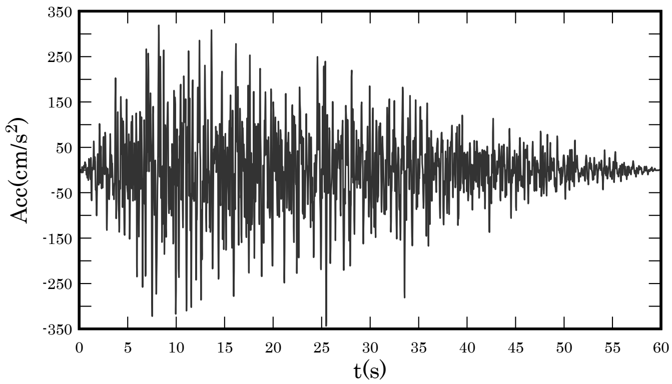

b)

Figure 10. a) Sinthesized accelerogram b) EC-8 soil type B, elastic design spectrum and response spectra

4. SEISMIC SAFETY OF THE BUILDINGS

4.1. Calculation of the performance point

As the main objective of this paper is to study the seismic safety of buildings designed according to the Eurocodes, it is necessary to define a measure of the engineering demand. The global drift of the structure corresponding to the performance point has been selected herein to assess the seismic safety of the buildings.

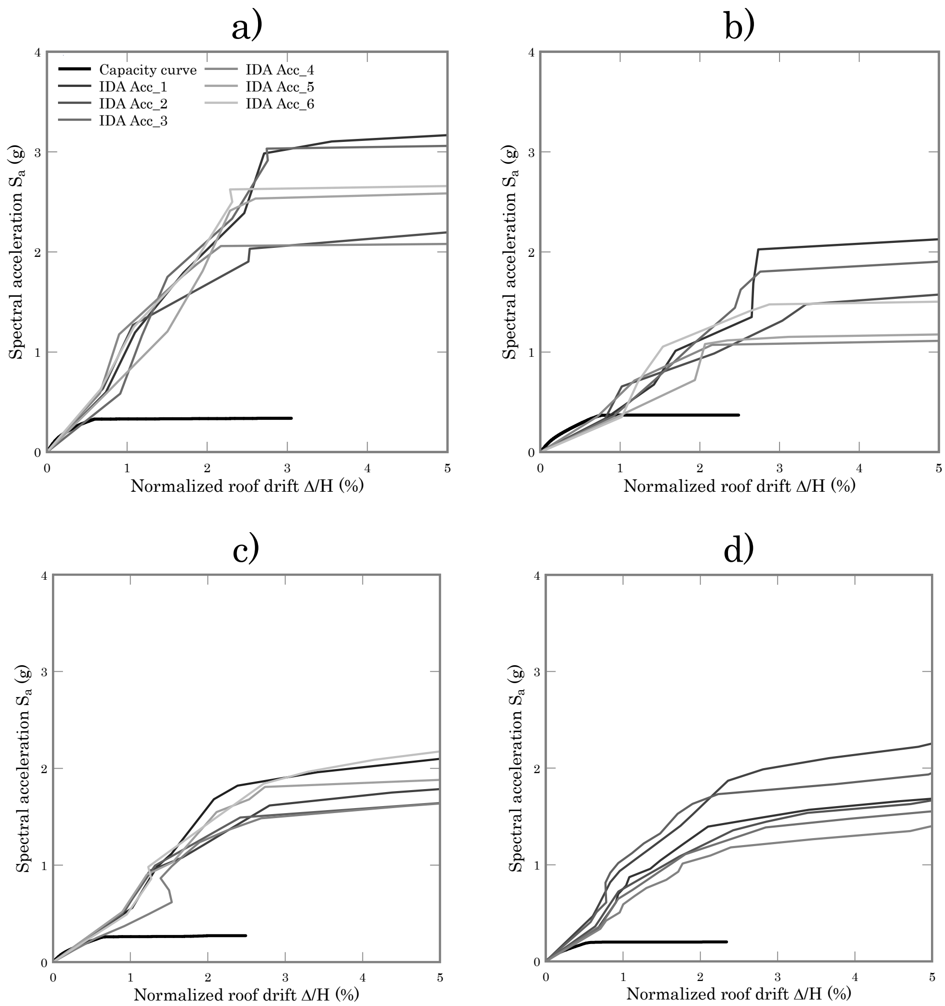

Figure 11. IDA curves of the a) WSB b) FBFB c) MRFB (EHE) and d) MRFB (EC)

Table 1. Normalized roof displacement (%) at the collapse of the structures

	Static analysis	Dynamic analysis (average)
3	2.51	2.51
6	2.63	2.63
9	2.48	2.62
12	2.35	2.39

Table 2. Behavior factors of the buildings

	$q_{equation}$ (Average)	q_{code}	$q_{equation}/q_{code}$
3	17.40	5.85	2.97
6	10.79	5.85	1.84
9	15.07	5.85	2.57
12	15.12	5.85	2.58

The performance point permits establishing the point of maximum drift of an equivalent single degree of freedom model induced by the seismic demand. It is determined in the paper by using the N2 procedure [30] which N2 requires transforming the capacity curve into a capacity spectrum expressed in terms of the spectral displacements S_d and of the spectral acceleration S_a; S_d is obtained by

$$S_d = \frac{\delta_c}{MPF} \tag{6}$$

where δ_c is the roof displacement and *MPF* the modal participation factor obtained from the response of the first mode of vibration

$$MPF = \frac{\sum_{i=1}^{n} m_i \phi_{1,i}}{\sum_{i=1}^{n} m_i \phi_{1,i}^2} \tag{7}$$

In this equation, m_i is the mass I and $\phi_{I,I}$ is the spectral ordinate. The spectral acceleration S_a is given by

$$S_a = \frac{V/W}{\alpha} \tag{8}$$

where V is the base shear, W is the seismic weight α and is the coefficient

$$\alpha = \frac{\left(\sum_{i=1}^{n} m_i \phi_{1,i}\right)^2}{\sum_{i=1}^{n} m_i \phi_{1,i}^2} \tag{9}$$

INTERSECTII
INTERSECTIONS
www.intersections.ro

Figure 12 shows the capacity spectra for the outer frame of the building with 3 stories and 3 spans, crossed with the corresponding demand elastic spectra. The idealized bilinear form of the capacity spectrum is also shown in the figure.

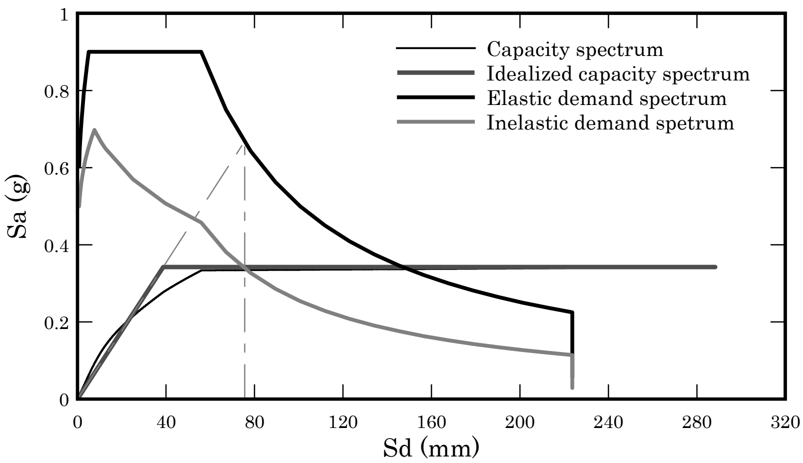

Figure 12. Capacity and demand spectra allowing the determination of the performance point of the outer frame of the building with 3 spans and 3 stories

The values of the spectral displacements corresponding to the performance point are shown in Table 3. An important feature in the non linear response of the buildings is the ratio between the performance point displacement and the ultimate displacement. This ratio indicates whether the behavior of a structure is ductile or fragile. The lower values of this ratio correspond to the 12 story building, which has a weak-beam strong-column failure mechanism.

Table 3. Roof drift of performance points for the studied buildings

	Normalized roof drift (%)			Ratio	
Story number	Performance point %)	Static analysis	Dynamic analysis (average)	Static analysis	Dynamic analysis (average)
3	0.80	3.02	2.51	0.26	0.32
6	0.51	2.48	2.63	0.20	0.19
9	0.39	2.48	2.62	0.16	0.15
12	0.21	2.34	2.39	0.09	0.09

ISSN 1582-3024

4.2. Fragility curves and damage probability matrices

The damage thresholds are determined using the VISION 2000 procedure [31] which expresses the thresholds in function of the interstory drift. In this work, five damage states thresholds are defined using both the interstory drift curve and the capacity curve. The *slight* damage state corresponds to the roof drift for which the first plastic hinge appears. The *moderate* damage state corresponds to the roof drift for which an interstory drift of 1% is reached in all the stories of the structure. The *repairable* damage state is defined by a interstory drift of 2%. The *severe* damage state is identified by a roof drift producing a 2,5% of interstory drift at each of the levels of the structure. Finally, the total damage state (collapse) corresponds to the ultimate roof displacement obtained from the capacity curve. Mean values and standard deviation were computed from the non linear response of buildings having the same geometry and structural type, by varying the number of spans from 3 to 6 in the *x* direction [32, 33].

The fragility curves are obtained by using the spectral displacements determined for the damage thresholds and considering a lognormal probability density function for the spectral displacements which define the damage states [34]

$$F(S_d) = \frac{1}{\beta_{ds} S_d \sqrt{2\pi}} \exp\left[-\frac{1}{2}\left(\frac{1}{\beta_{ds}} \ln \frac{S_d}{\bar{S}_{d,ds}} \right)^2 \right] \tag{10}$$

where $\bar{S}_{d,ds}$ is the mean value of the spectral displacement for which the building reaches the damage state threshold d_s and β_{ds} is the standard deviation of the natural logarithm of the spectral displacement for the damage state d_s. The conditional probability $P(S_d)$ of reaching or exceeding a particular damage state d_s, given the spectral displacement S_d, is defined as

$$P(S_d) = \int_0^{S_d} F(S_d) d(S_d) \tag{11}$$

Figure 13 shows the fragility curves calculated for the four different heights of buildings considered in the analysis.

ISSN 1582-3024

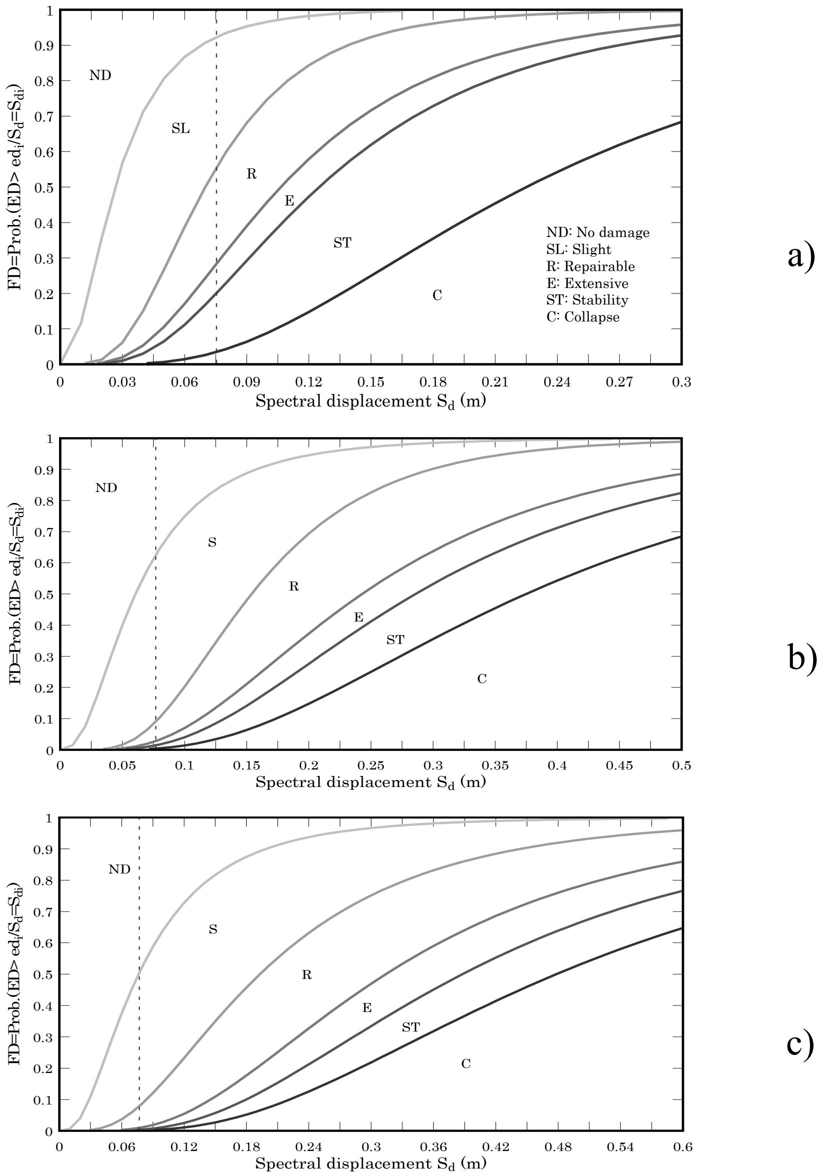

ISSN 1582-3024

INTERSECTII
INTERSECTIONS
www.intersections.ro

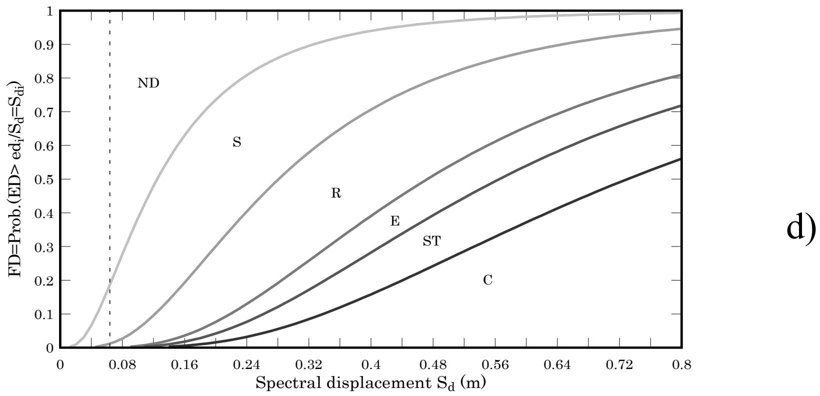

Figure 13. Fragility curves of the a) 3 story, b) 6 story, c) 9 story and d) 12 story buildings

Figure 14 shows the damage probability matrices calculated for the performance points corresponding to all the studied cases. It is worth to observe that the probabilities are not sensitive to the variation of the span number. It is also important to note that for the frames of the same building, the probabilities vary according to the load ratio (seismic load/gravity load).

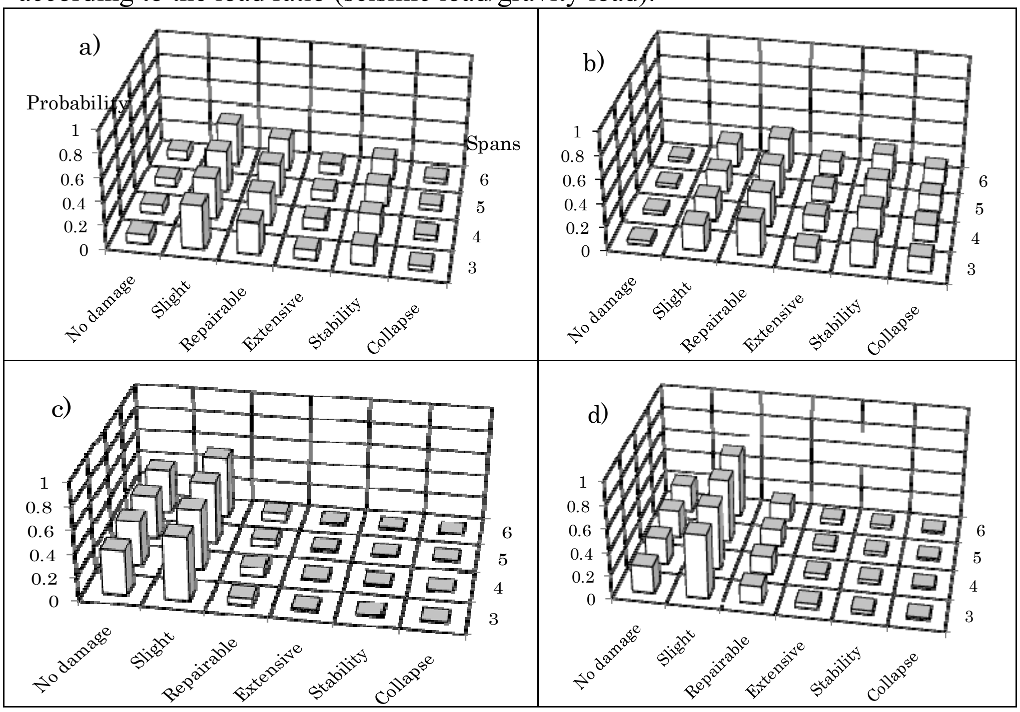

ISSN 1582-3024

INTERSECTII
www.intersections.ro

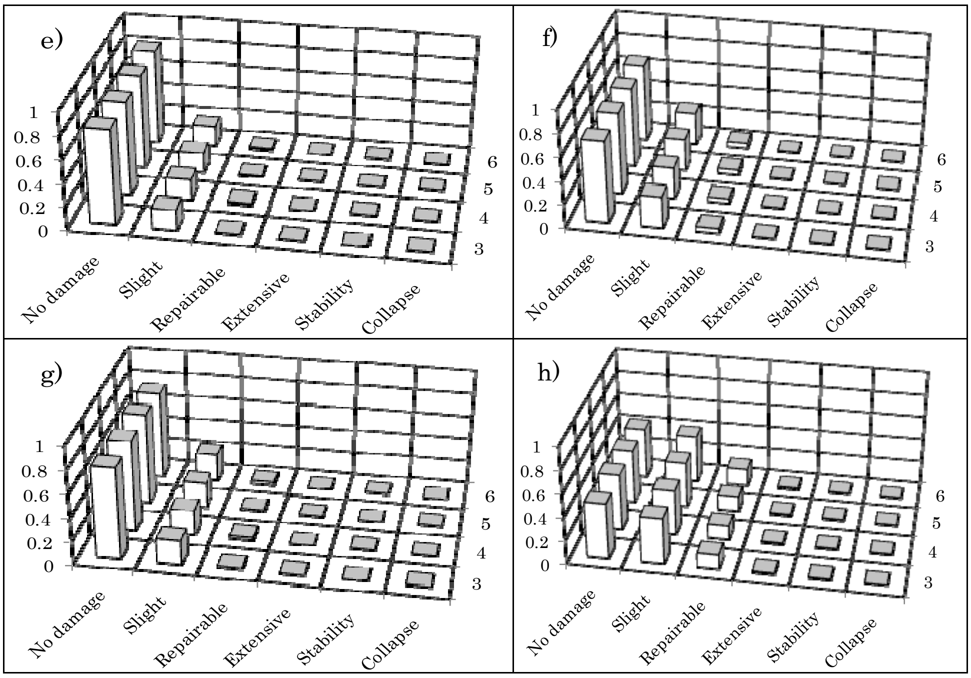

Figure 14. Damage probability matrices of a) outer and b) inner frames of 3 story buildings, c) outer and d) inner frames of 6story buildings, e) outer and f) inner frames of 9 story buildings and g) outer and h) inner frames of 12 story buildings

Another important feature which can be observed in the obtained results is the increase of the probability values that correspond to the higher damage states for low rise buildings, for which the collapse is associated to the soft-storey mechanism as discussed in previous sections. For example, in the case of the inner frames of the 3 levels building, the probability to reach the *collapse* is four times higher than in the case of the outer frames of the same building. In contrast, the 6, 9 and 12 story buildings show very low probabilities to reach more severe damage states regardless of the load ratio and of the span number. For these buildings, the predominant damage states are the *non-damage* and the *slight* damage.

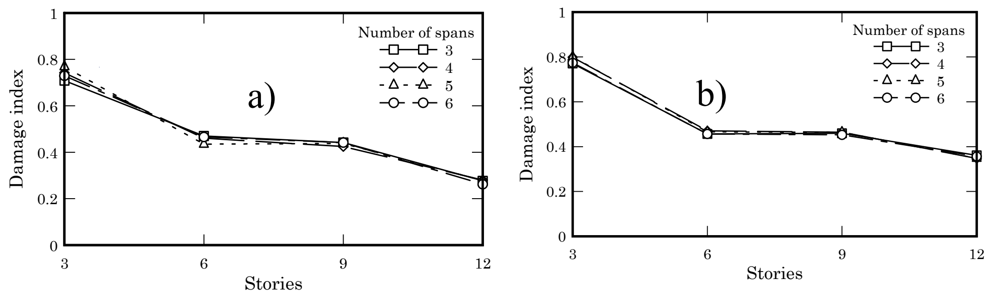

Figure 14. Damage index computed for the a) outer frames and b) inner frames

Figure 14 shows the values of the damage index correspondingto the performance point of the different frames. These values were obtained using Eq. 3. First of all, it is possible to observe that low rise buildings (3 levels) reach high values of the damage index than the other buildings; this is a consequence of the failure mechanism which occurs for this kind of buildings (soft story mechanism). In contrast, the 12 levels buildings exhibits damage index about 0.3 to 0.35 for the outer frames, values that are consistent with the failure mechanism (strong columns-weak beams) and with the probabilities obtained from the fragility curves. Finally it is important to observe that the values of the damage index of the outer frames are lower than the values of the damage index of the inner frames, indicating that the damage index depends on the load type ratio.

5. CONCLUSIONS

- The Incremental Dynamic Analysis is useful in order to assess the collapse threshold of the frames. The dynamic analysis, which is also suitable for the evaluation of the behavior factor q, confirms the values obtained by means of the pushover analysis.
- The local damage distribution of the buildings corresponding to the collapse threshold shows that low rise buildings have a failure mechanism associated to the formation of the soft storey mechanism. Medium rise buildings (6, 9 and 12 story) exhibit a failure mechanism associated to the weak-beam and strong-column conceptual design objective.
- Reinforced concrete framed buildings, designed according to the Eurocodes for a high ductility class, exhibit adequate values of overstrength which are greater than the value prescribed in the code (1.5). Behavior factors obtained by means of the dynamic analysis are also adequate and are twice the code values. In the procedure applied to evaluate such factors, no influence of the structural redundancy was detected.

- Generally speaking, the studied buildings show adequate ductility behavior, as it is evidenced by the displacement ductility values and by the ratio between the performance point and the ultimate displacement.
- The nonlinear response of the buildings depends on the ratio between the seismic and gravity loads. The inner frames which are designed for lower ratios have lower overstrength values. Consequently, the seismic safety of the different frames is influenced by this ratio.
- The assessment of the seismic safety of the buildings demonstrates that low rise buildings reach higher damage states than the other studied buildings, when they are subjected to the demand prescribed by the elastic design spectrum. This fact is a consequence of the failure mechanism of the low rise buildings. The probability of damage is not sensitive to the span number of the frames.
- The proposed objective damage index predicts adequately the state of damage that is achieved by the frames for a specific seismic demand value (displacement of the performance point).

Acknowledgements

Most of the developments included in this work are consequence of several research projects. The institutions and companies responsible of these projects are gratefully acknowledged. These are, CEE–FP6 (LESSLOSS project, ref. FP6-50544(GOCE)); the Spanish Goverment through the Ministerio de Ciencia y Tecnología (RECOMP project, ref. BIA2005-06952, DECOMAR project, ref. MAT2003-08700-C03-02 and DELCOM project, ref. MAT2008-02232/MAT) and the Ministerio de Fomento (project "Retrofitting and reinforcement of reinforced concrete structures with composite materials. Numerical and experimental developments applied to joint of bars and composites anchorage proposal"); AIRBUS through the project FEMCOM and ACCIONA Infraestructuras through the projects SPHERA, CETIC, PROMETEO.

References

1. Mwafi, A.M. Elnashai, A. Overstrength and force reduction factors of multistory reinforced-concrete buildings, *Structural design of tall buildings*, **11**, 329-351, 2002.
2. Mwafi AM, Elnashai A. Calibration of force reduction factors of RC buildings, *Journal of Earthquake Engineering*, **6(2)**, 239-273, 2002
3. Sanchez, L. Plumier, A. Parametric study of ductile moment-resisting steel frames: a first step towards Eurocode 8 calibration, *Earthquake engineering and structural dynamics*, **37**, 1135-1155, 2008.
4. Comité Européen de Normalisation (CEN). *Eurocode 2: Design of concrete structures. BS EN 1992*, Brussels, 2001.
5. Comité Européen de Normalisation (CEN). *Eurocode 8: Design of Structures for Earthquake Resistance. EN 2004-1-1*, Brussels, 2003.

6. PLCd Manual. Non-linear thermo mechanic finite element oriented to PhD student education, code developed at CIMNE, Barcelona, Spain, 2009.
7. Oller, S. and Barbat, A. H. (2006). Moment-curvature damage model for bridges subjected to seismic loads, *Computer Methods in Applied Mechanics and Engineering*, **195**, 4490-4511, 2006.
8. Car, E., Oller, S. and Oñate, E. A large strain plasticity for anisotropic materials: Composite material application, *International Journal of Plasticity*, **17(11)**, 1437-1463, 2001.
9. Mata, P., Oller, S. and Barbat, A.H. Static analysis of beam structures under nonlinear geometric and constitutive behaviour, *Computer Methods in Applied Mechanics and Engineering*, **196**, 4458-4478, 2007
10. Mata, P., Oller, S. and Barbat, A. H. Dynamic analysis of beam structures under nonlinear geometric and constitutive behaviour, *Computer Methods in Applied Mechanics and Engineering*, **197**, 857-878, 2008.
11. Oller S, Onate E, Oliver J, Lubliner J. Finite element non-linear analysis of concrete structures using a plastic-damage model, *Engineering Fracture Mechanics*, **35(1–3)**, 219–31, 1990.
12. Lubliner, J. Oliver, J. Oller, S. Oñate, E. A plastic-damage model for concrete, *International Journal of Solids & Structures*, **25(3)**, 299–326, 1989
13. Barbat, A.H. Oller, S. Onate, E. Hanganu, A. Viscous damage model for Timoshenko beam structures, *International Journal of Solids & Structures*, **34(30)**, 3953–76, 1997.
14. Faleiro, J. Oller, S. Barbat, A.H. Plastic-damage seismic model for reinforced concrete frames, *Computer and Structures*, **86**, 581–97, and 2008.
15. Oller S., Car E., Lubliner J. Definition of a general implicit orthotropic yield criterion, *Computer Methods in Applied Mechanics and Engineering*, **192(7–8)**, 895–912, 2003.
16. Martinez, X. Oller, S. Rastellini, F. Barbat, A.H. A numerical procedure simulating RC structures reinforced with FRP using the serial/parallel mixing theory, *Computers and Structures*, **86**, 1604–1618, 2008.
17. Bayrak O., Sheikh SA. Plastic hinge analysis, *Journal of Structural Engineering*; **127**, 1092–100, 2004.
18. Spacone E, El-Tawil S. Nonlinear analysis of steel–concrete composite structures: State of the art, *Journal of Structural Engineering,* **126**, 159–68, 2000.
19. Shao Y, Aval S, Mirmiran A. Fiber–element model for cyclic analysis of concrete-filled fiber reinforced polymer tubes, *Journal of Structural Engineering,* **131**, 292–303, 2005.
20. Simo, J.C. A finite strain beam formulation. The three-dimensional dynamic problem. Part I. *Computer Methods in Applied Mechanic and Engineering*, 49:55–70, 1985.
21. Mander, J. B., Priestley, M.J. N. y Park, R. Observed stress-strain behaviour of confined concrete, *Journal of Structural Engineering*, **114**, 1827-1849, 1988.
22. Priestley, M.J.N. Calvi, G.M. Kowalsky, M.J. *Displacement-based seismic design of structures*. IUSS Press. Pavia, Italy, 2007.
23. Park, R. State-of-the-art report: ductility evaluation from laboratory and analytical testing, *Proceedings 9th WCEE, IAEE*, Tokyo-Kyoto, Japan, 605-616, 1988.
24. Barbat, A. H. Oller, S. Oñate, E. Hanganu, A. Viscous damage model for Timoshenko beam structures, *International Journal of Solids and Structures*, **34(30)**, 3953-3976, 1997.
25. Car, E., Oller, S. and Oñate, E. An anisotropic elastoplastic constitutive model for large strain analysis of fiber reinforced composite materials, *Computer Methods in Applied Mechanics and Engineering*, **185(2-4)**, 5-277, 2000.
26. Vielma, J. C. Barbat, A. H. Oller, S. Un índice de daño objetivo para la evaluación de los edificios de hormigón armado. *Hormigón y acero*. **248**, 53-64, 2007.
27. Vamvatsikos. D, Cornell, C.A. Incremental dynamic analysis, *Earthquake Engineering and Structural Dynamics*, **31(3)**, 491-514, 2002.
28. Kunnath, S. *Performance-based seismic design and evaluation of buildings structures. In: Chen W and Lui E (ed). Earthquake engineering for structural design*, CRC Press. Boca Raton, 2005.
29. Han, S.W. Chopra, A. Approximate incremental dynamic analysis using the modal pushover analysis procedure, *Earthquake Engineering and Structural Dynamics*, 35(3): 1853-1873, 2006.

ISSN 1582-3024

INTERSECTII
www.intersections.ro
INTERSECTIONS

30. Fajfar, P. A. Nonlinear Analysis Method for Performance Based Seismic Design, *Earthquake Spectra*, **16(3)**, 573-591, 2000.
31. SEAOC. *Vision 2000 Report on Performance Based Seismic Engineering of Buildings*, Structural Engineers Association of California, Volume I, Sacramento, California, 1995.
32. Vielma, J. C., Barbat, A. H. y Oller, S. Umbrales de daño para estados límite de edificios porticados de concreto armado diseñados conforme al ACI-318/IBC-2006, *Revista Internacional de Desastres Naturales, Accidentes e Infraestructura*, 8(2), 119-133, 2008.
33. Vielma, J. C. *Caracterización de la respuesta sísmica de edificios de hormigón armado mediante la respuesta no lineal*, PhD Thesis, Barcelona, **ISBN**: 978-84-691-3475-7, 2008.
34. Pinto, P.E. Giannini, R. Franchin, P. Seismic reliability analysis of structures. IUSS Press, Pavia, Italy. 2006.

ISSN 1582-3024